Cancer Research

Extracellular Vesicles Modulate the Glioblastoma Microenvironment via a Tumor Suppression Signaling Network Directed by miR-1

Agnieszka Bronisz[1,4], Yan Wang[3], Michal O. Nowicki[1,3], Pierpaolo Peruzzi[3], Khairul I. Ansari[1], Daisuke Ogawa[1,3], Leonora Balaj[2], Gianluca De Rienzo[1], Marco Mineo[1], Ichiro Nakano[3], Michael C. Ostrowski[4], Fred Hochberg[2], Ralph Weissleder[2], Sean E. Lawler[1,3], E. Antonio Chiocca[1,3], and Jakub Godlewski[1,3]

Abstract

Extracellular vesicles have emerged as important mediators of intercellular communication in cancer, including by conveying tumor-promoting microRNAs between cells, but their regulation is poorly understood. In this study, we report the findings of a comparative microRNA profiling and functional analysis in human glioblastoma that identifies miR-1 as an orchestrator of extracellular vesicle function and glioblastoma growth and invasion. Ectopic expression of miR-1 in glioblastoma cells blocked *in vivo* growth, neovascularization, and invasiveness. These effects were associated with a role for miR-1 in intercellular communication in the microenvironment mediated by extracellular vesicles released by cancer stem–like glioblastoma cells. An extracellular vesicle–dependent phenotype defined by glioblastoma invasion, neurosphere growth, and endothelial tube formation was mitigated by loading miR-1 into glioblastoma-derived extracellular vesicles. Protein cargo in extracellular vesicles was characterized to learn how miR-1 directed extracellular vesicle function. The mRNA encoding Annexin A2 (ANXA2), one of the most abundant proteins in glioblastoma-derived extracellular vesicles, was found to be a direct target of miR-1 control. In addition, extracellular vesicle–derived miR-1 along with other ANXA2 extracellular vesicle networking partners targeted multiple pro-oncogenic signals in cells within the glioblastoma microenvironment. Together, our results showed how extracellular vesicle signaling promotes the malignant character of glioblastoma and how ectopic expression of miR-1 can mitigate this character, with possible implications for how to develop a unique miRNA-based therapy for glioblastoma management. *Cancer Res; 74(3); 738–50. ©2013 AACR.*

Introduction

Glioblastoma multiforme, the most common and aggressive primary brain tumor, is diagnosed in approximately 10,000 new cases per year in the United States (1), with a median survival of approximately 14 months (2). Glioblastoma multiforme is characterized by cellular heterogeneity, rapid proliferation, angiogenesis, and extensive invasion (3). Concomitant high proliferation and infiltration constitutes the major challenge for glioblastoma multiforme therapy because even with extensive resection tumor cells are left behind in the brain, leading to recurrence. Angiogenesis constitutes a major advantage to rapidly growing tumors by providing oxygen and nutrients, yet antiangiogenic treatment may paradoxically increase invasiveness (4). Thus, novel therapies aimed at blocking glioblastoma multiforme growth, as well as curbing its invasive and angiogenic potential, are needed.

Glioblastoma multiforme displays a high level of intratumoral cellular heterogeneity and has been shown to contain subpopulations of tumorigenic cells with stem cell–like properties (5). The tumor vasculature provides a specialized niche for stem-like tumor cells (6). Moreover, these tumors modify normal cells in their environment to promote tumorigenicity in various ways (7) and tumor-associated cells such as vascular cells, microglia, peripheral immune cells, and neural precursors also play important roles in the microenvironment (8). Increasing evidence shows that a crucial mode of cell–cell communication within tumors is the release and uptake of small extracellular vesicles that contain a subset of cellular proteins and RNAs (9, 10). Extracellular vesicles are taken up by cells and can change their phenotype by delivery of tumor-derived RNAs, including

Authors' Affiliations: [1]Harvey Cushing Neuro-oncology Laboratories, Department of Neurosurgery, Brigham and Women's Hospital, Harvard Medical School, Boston; [2]Neuroscience Center at Massachusetts General Hospital, Charlestown, Massachusetts; Departments of [3]Neurological Surgery and [4]Molecular and Cellular Biochemistry, The Ohio State University Medical Center, Columbus, Ohio

Note: Supplementary data for this article are available at Cancer Research Online (http://cancerres.aacrjournals.org/).

A. Bronisz and Y. Wang contributed equally to this work.

Corresponding Authors: Jakub Godlewski, Brigham and Women's Hospital, Harvard Medical School, 4 Blackfan Circle, Boston, MA 02115. Phone: 617-5255060; Fax: 617-5255067; E-mail: jgodlewski@partners.org; and E. Antonio Chiocca, Brigham and Women's Hospital, Harvard Medical School, 75 Francis Street, Boston, MA 02115. Phone: 617-732-6939; Fax: 617-734-8342; E-mail: EAChiocca@partners.org

doi: 10.1158/0008-5472.CAN-13-2650

microRNAs (miR; ref. 11). In recent years, numerous reports suggested an important role for extracellular vesicle communication in glioblastoma multiforme, including the transfer of miRs (9, 12, 13).

miRs are small, noncoding RNAs that act as regulators of gene expression by reducing translation of target mRNAs with partial complementarity in their 3′-untranslated regions (UTR; ref. 14). miR deregulation is a general feature of cancer, including glioblastoma multiforme, and is associated with both tumor suppressor and oncogenic effects (15, 16).

miR-1 has been shown to function as a tumor suppressor in several human cancers (17). In this study, we report that miR-1 is novel tumor suppressor in glioblastoma multiforme. We describe multilevel antitumorigenic effects of miR-1 restoration, including signaling by extracellular vesicles. Multiple oncogenic signaling pathways were inactivated by miR-1, showing the distinctive ability of a single miR to simultaneously inhibit numerous targets, both directly and indirectly. Moreover, we show that the pro-oncogenic effect of glioblastoma multiforme–derived extracellular vesicles was alleviated by miR-1, which directly targets Annexin A2 (ANXA2), one of the most abundant extracellular vesicle proteins. ANXA2 is upregulated in various tumor types (18), including glioblastoma multiforme (19) where it plays a critical role in driving invasion and progression (20). Our results show that miR-1 delivery reduces glioblastoma multiforme tumorigenicity and impairs extracellular vesicle–based microenvironmental communication, suggesting that such communication may be a candidate for therapeutic treatment of glioblastoma multiforme.

Materials and Methods

Human specimens

All tumor samples were obtained as approved by the Institutional Review Board at The Ohio State University (OSU; Columbus, OH). Surgery was conducted by E.A. Chiocca or I. Nakano. For each patient, samples of both tumor and adjacent brain devoid of gross tumor were processed for extraction of total RNA (TRIzol, Invitrogen) and protein (Cell Lysis Buffer, Cell Signaling) or establishment of patient-derived neurospheres.

Cell culture

U87, U251, U373, Gli36 malignant glioblastoma multiforme (American Type Culture Collection) were cultured in Dulbecco's Modified Eagle Medium (DMEM; Invitrogen) with 10% or 2% fetal calf serum (FCS, Sigma). Human brain microvessel endothelial cells (HBMVEC; Cell System) were cultured in endothelial cell basal medium supplemented with 1% endothelial cell growth supplement and 5% FBS. The normal human astrocytes (NHA, Clonetics) were cultured in astrocyte basal medium supplemented with 1% astrocyte growth supplement and 2% FBS (Lonza). Primary human glioblastoma multiforme cells X12 were obtained as previously reported (21, 22). For neurosphere culture, cells were grown in stem cell medium, consisting of Neurobasal/Glutamax (Invitrogen) supplemented with 1% N2 and 2% B27 (Invitrogen) and 20 ng/mL EGF and fibroblast growth factor-2 (PeproTech). Cells were grown as adherent monolayers in poly-L-ornithine and laminin-covered dishes (Invitrogen) and as neurospheres in stem cell medium.

Vector construction and transfection

The lentiviral pCDH-GFP empty vector and miR-1-1–expressing vector were purchased from System Biosciences. The lentiviral constructs along with lentiviral packaging constructs were used for establishing U87 and X12 cell lines constitutively overexpressing GFP or GFP/miR-1, according to the manufacturer's instruction. For each construct, 3 independent clones were created and expression of miR-1 was validated by quantitative PCR (qPCR). The RFP CD63 lentiviral particles from System Bioscience were used for creating U87 and X12 cell lines overexpressing RFP CD63.

The 3′-UTR encompassing the target sequence for miR-1 of *ANXA2* cDNA were cloned into the pMIR-REPORT vector (Ambion). For the mutated, construct of the QuickChange Site-Directed Mutagenesis Kit (Stratagene) was used according to manufacturer's protocol to alter the miR-1 seed sequence. Luciferase reporter assays were conducted as previously described (23) using luciferase reagent (Promega). Extracellular vesicles loaded with miR (NC or miR-1) were used for luciferase assays at a concentration of 500 extracellular vesicles per cell. Cells were treated with extracellular vesicles 24 hours before reporter transfection. Transfection (25–75 nmol/L) of negative control (NC) and pre-miR-1 (miR-1) or pre-miR-1 FAM labeled (miR-1 FAM; Ambion) or pMIR-REPORT was done with Lipofectamine 2000 (Invitrogen).

In vivo studies

Female immunodeficient mice were purchased from Taconic. For all studies, the mice were housed in animal facility at the OSU in accordance with all NIH regulations. All protocols were approved by the OSU Institutional Animal Care and Use Committee. *In vivo* studies were conducted as previously described (see Supplementary Experimental Procedures; ref. 24). Tumors from flank and brains were placed in 4% paraformaldehyde for 24 hours and then in 30% sucrose for 48 hours. Sections of 20 μm were evaluated for Ki67 (Abcam), cleaved caspase-3 (Cell Signaling), CD31 (BD Pharminogen), and lectin (Invitrogen) immunostaining or green/red fluorescence. For quantification of staining/fluorescence, 3 sections per tumor were analyzed.

In vitro 2- and 3-dimensional assays

Three-dimensional (3D) spheroid migration assay in collagen matrix and its quantification were conducted as previously described (23). The vessel-forming ability of HBMVECs was characterized *in vitro* using a Matrigel assay (see Supplementary Experimental Procedures; ref. 25). Propidium iodide exclusion and flow cytometry–based cell-cycle analysis was carried out using the Becton Dickinson FACSCalibur System.

Purification of extracellular vesicles

To isolate extracellular vesicles, U87 and X12 cells were cultured for 2 days in extracellular vesicle–free medium without antibiotics. The conditioned media were collected and extracellular vesicles were isolated by differential centrifugation as previously described (see Supplementary Experimental Procedures; ref. 26).

Proteomic analysis

All mass spectra were acquired at the Bioproximity LLC. Proteins were prepared for digestion using the filter-assisted sample preparation (FASP) method (see Supplementary Experimental Procedures; ref. 27).

Protein extraction and Western blot analysis was done as described previously (28). Representative images from 2 or 3 independent experiments are shown. Antibodies used were as follows: ANXA2 (1:1,000, Santa Cruz), CD133 (1:1,000, Amersham), BMI1 and GFAP (1:1,000, Millipore), Akt and pAKT Ser473, ERK and pERK Thr202/Tyr204Y, JNK and pJNK Thr183/Tyr185, MET and p-MET Tyr1234/1235, EGFR, PDGFRA, SUZ12, FASN (1:2,000, Cell Signaling), YWHAZ and CD63 (1:1,000, Santa Cruz), CD9 (1:500, Novus), and α-tubulin (1:10,000, Sigma-Aldrich).

Microscopy

All fluorescent and light microscopy–based assays were monitored using a Zeiss LSM510 confocal microscope system (Carl Zeiss Inc.). Ultrathin frozen sections and immunogold-labeled CD63 antibody were prepared in Cellular Neuroscience Core Laboratory. The Transmission Electron microscopy Tecnai G^2 Spirit BioTWIN or with AMT 2k CCD camera was used to analyze extracellular vesicles stained with immunogold-labeled anti-CD63 antibody in Electron Microscopy Facility at Harvard Medical School (Boston, MA).

Quantitative PCR

Total RNA was extracted using TRIzol (Invitrogen) and treated with RNase-free DNase (Qiagen). Mature and pri-miR expression analysis by qPCR was carried out using the miR Real-Time PCR Detection Kit (Applied Biosystems) as described (23). mRNA expression analysis was conducted using Power SYBR Green (Applied Biosystems). RNA concentration was quantified using Nanodrop RNA 6000 nano-assays and analyzed using Agilent 2100 Bioanalyzer total and Pico RNA platform.

Data and statistical analysis

All microscopy-based assays were edited/quantified using ImageJ (http://rsb.info.nih.gov.ezp-prod1.hul.harvard.edu/ij/), including the Analyze Skeleton plugin and Analyze Particles function of binary images with automatic threshold. Pathway analysis was conducted using Ingenuity Pathways Analysis (IPA, http://www.ingenuity.com/) and David Functional Annotation tools (http://david.abcc.ncifcrf.gov/). Results are expressed as mean ± SD, and differences were compared using the 2-tailed Student *t* test. Statistical analyses were conducted using Microsoft Office Excel 2010 or GraphPad Prism 6 software. $P < 0.05$ was considered statistically significant (single asterisks in the figures), and $P < 0.01$ was strongly significant (double asterisks).

Results

miR-1 is downregulated in human glioblastoma multiforme and in glioblastoma multiforme cells during migration *in vitro*

Our previously published microarray study indicated that miR-1 levels were significantly reduced when compared with adjacent brain tissue from the same individual (29). More recently, our group also showed that the expression of miR-1 was shut off over a 3-day *in vitro* spheroid migration assays (23). In fact, miR-1 was 1 of 5 miRs downregulated in both arrays (Fig. 1A). To validate the microarray data from the first study (29), we tested miR-1 expression in a panel of 8 patient glioblastoma multiforme samples with matched adjacent brain by quantitative real-time (Fig. 1B). This confirmed that there was significant downregulation of miR-1 in glioblastoma multiforme compared with surrounding brain. The microarray

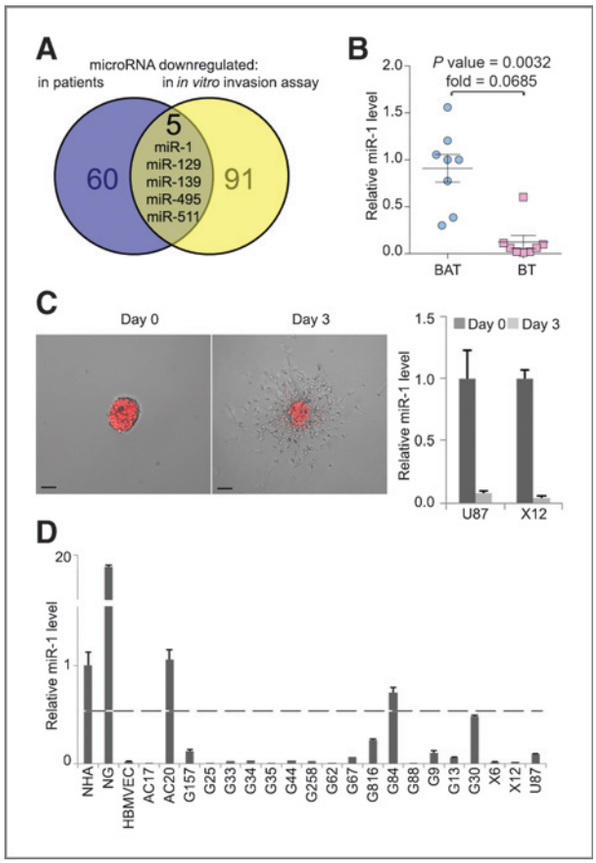

Figure 1. miR-1 is downregulated in patient glioblastoma multiforme specimens and in glioblastoma multiforme cells during migration *in vitro*. A, Venn diagram depicting the overlap between miRs identified as downregulated in glioblastoma multiforme specimens compared with matching (i.e., from the same individual) adjacent brain (blue) and miRs identified as downregulated in glioblastoma multiforme cells in time course of a migration assay (yellow). B, relative expression of miR-1 was validated by qPCR in glioblastoma multiforme brain tumor (BT) specimens versus matching brain adjacent to tumor (BAT; $n = 8$). Values, mean relative miR-1 expression level ± SD. C, representative images of RFP-X12 glioblastoma multiforme cells in the migration assay at days 0 and 3 are shown. RNA was extracted from multiple spheroids for subsequent analysis. Scale bars, 200 μm. Relative expression of miR-1 was validated by qPCR in U87 and X12 glioblastoma multiforme cell lines at days 0 and 3 of migration in the spheroid assay. Values, mean relative miR-1 expression level ± SD. D, relative expression of miR-1 was validated by qPCR in normal human astrocytes (NHA), neuroglia (NG), HBMVECs, and collection of glioblastoma multiforme primary stem cells and established cell line U87. Values, mean relative miR-1 expression level ± SD. Dashed line, 50% of expression measured in astrocytes.

data from the second study (23) were also validated by showing that miR-1 was downregulated in U87 and X12 glioblastoma multiforme cells during a 3-day migration assay (Fig. 1C). Finally, we assessed miR-1 expression in nonmalignant astrocytes, neuroglia, and endothelial brain microvasculature, as well as in a broad panel of glioblastoma multiforme–derived cell lines (primary glioblastoma multiforme stem–like cells from grade III and IV tumors, and established glioblastoma multiforme cell lines). Expression was moderate in astrocytes, high in neuroglia, and very low in endothelial cells. In 17 of 20 malignant cell lines, miR-1 expression was low or undetectable (Fig. 1D). The identification of low levels of miR-1 in tumor tissue and tumor cells, as well as a reduction in migrating cells strongly suggests that miR-1 may play a tumor-suppressive role in glioblastoma multiforme.

Overexpression of miR-1 in glioblastoma multiforme cells reduces tumorigenicity, angiogenesis, and invasion *in vivo*

On the basis of the above findings, we hypothesized that miR-1 may act as a tumor suppressor. To investigate the function of miR-1 in glioblastoma, we stably expressed miR-1 using a lentiviral expression vector. U87 flank xenografts expressing miR-1 were significantly smaller than controls (Fig. 2A), and there was significant reduction in the proliferation index (Supplementary Fig. S1A). The decreased growth was not due to apoptosis because cleaved caspase-3 was not significantly elevated in cells expressing miR-1 (Supplementary Fig. S1B). Interestingly, the recruitment of endothelial cells measured by CD31 staining was significantly decreased, suggesting that impaired angiogenesis is at least partially responsible for

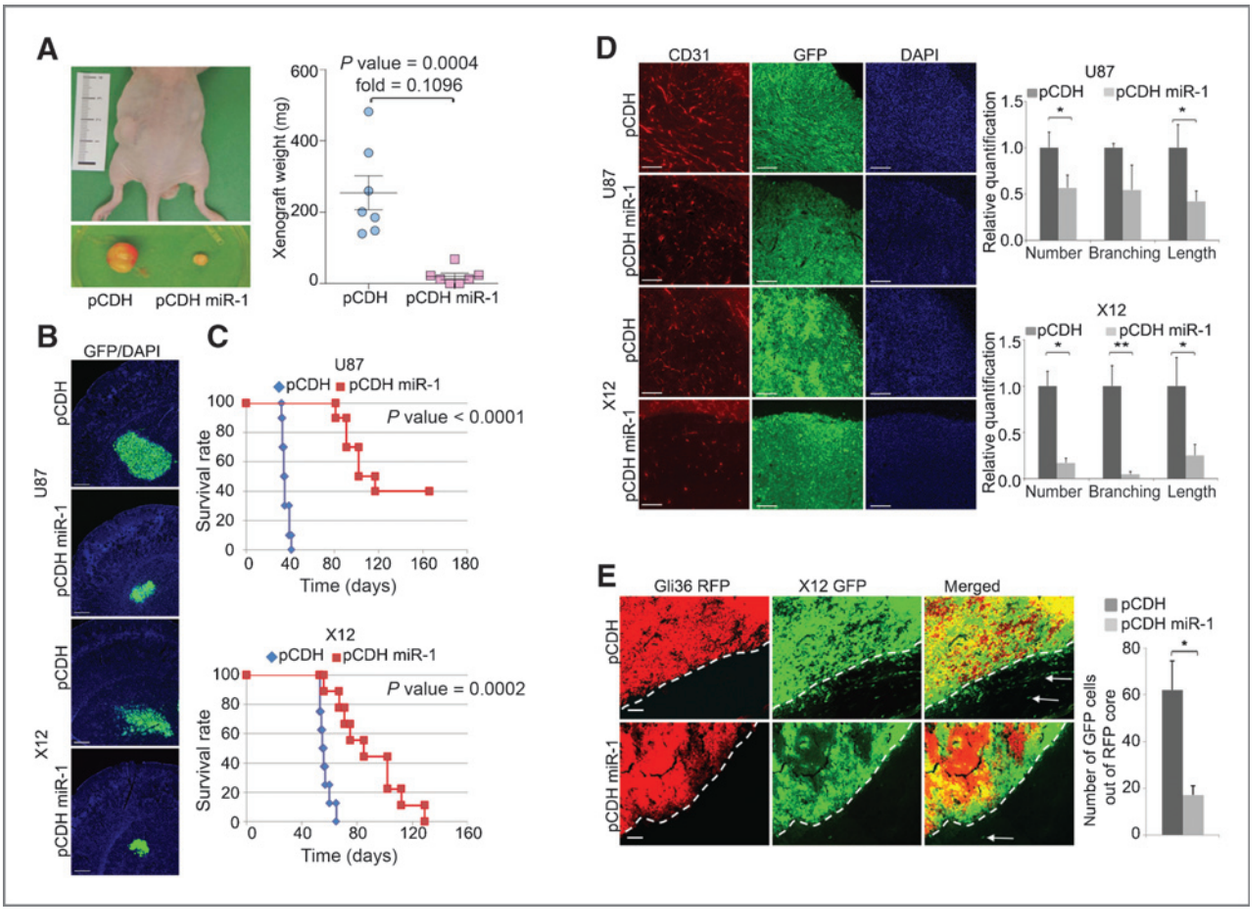

Figure 2. Overexpression of miR-1 in glioblastoma multiforme cells mitigates tumorigenicity, reduces invasiveness, and angiogenesis *in vivo*. A, representative images of tumor xenografts before and after excision from mice injected with U87 cells stably expressing pCDH-GFP control vector (pCDH) or pCDH-GFP miR-1 vector (pCDH miR-1). Tumor mass was quantified ($n = 7$), and the data are expressed as mean ± SD. B, representative images of intracranial tumors formed by U87 (2 weeks after injection) and X12 (3 weeks after injection) glioblastoma multiforme cells stably expressing pCDH-GFP control vector (pCDH) or pCDH-GFP miR-1 vector (pCDH miR-1). Scale bars, 250 μm. C, Kaplan–Meier survival curve of animals injected with glioblastoma multiforme tumor cells U87 (top) and X12 (bottom). Cells were stably expressing pCDH-GFP control vector (pCDH; U87, $n = 10$; X12, $n = 8$) or pCDH-GFP miR-1 vector (pCDH miR-1; U87, $n = 10$; X12, $n = 9$). Log-rank test was used to compare the survival probabilities between the two groups. D, angiogenesis was determined by CD31 (red) and DAPI (blue) staining of intracranial tumors formed by U87 (5 weeks after injection) and X12 (7 weeks after injection) glioblastoma multiforme cells stably expressing pCDH-GFP control vector (pCDH) or pCDH-GFP miR-1 vector (pCDH miR-1). Scale bars, 150 μm. Data, mean ± SD. *, $P < 0.05$; **, $P < 0.01$. E, invasiveness *in vivo* was determined by co-injection of noninvasive RFP-Gli36 cells with invasive GFP-X12 cells stably expressing either pCDH-GFP control vector (pCDH) or pCDH-GFP miR-1 vector (pCDH miR-1). Data quantified per random field. Scale bars, 100 μm. Data, mean ± SD; *, $P < 0.05$.

the observed growth inhibition mediated by miR-1 *in vivo* (Supplementary Fig. S1C). Next, we evaluated glioblastoma multiforme cell tumorigenicity by intracranial implantation of U87 and X12 cells stably expressing miR-1. These tumors were significantly smaller than controls (Fig. 2B). Survival analysis showed a significantly better outcome of animals injected with miR-1–expressing cells. In U87 cells we observed a substantial subgroup of long-term survivors (Fig. 2C). Analysis of neovascularization was conducted on symptomatic animals at 5 weeks (U87) or 7 weeks (X12) after tumor implantation. miR-1–expressing tumors displayed reduced CD-31 staining, with shorter average branch length and fewer prominent branches (Fig. 2D). These results were confirmed by lectin staining (Supplementary Fig. S1D). Finally, tumors formed by invasive X12 cells were smaller and also less diffusely infiltrative when miR-1 was expressed (Fig. 2B). To quantify invasiveness *in vivo*, noninvasive RFP-Gli36 cells were co-injected with invasive X12 cells stably expressing GFP alone or GFP/miR-1. Control X12 cells readily migrated out of the RFP-positive tumor core, whereas those expressing miR-1 were predominantly localized intratumorally (Fig. 2E). These results thus link miR-1 to a tumor suppressor role by inhibition of growth, invasiveness, and angiogenesis of glioblastoma multiforme.

Overexpression of miR-1 in glioblastoma multiforme cells impairs neurosphere formation and migration through multiple effectors

We became interested in exploring the effect of mR-1 on glioblastoma multiforme cell invasion. We first used *in vitro* adhesion assays and observed that miR-1–expressing cells were poorly adhesive, (Supplementary Fig. S2A) and cell-cell adhesiveness assays quantified the significance of this phenotype (Supplementary Fig. S2B). Indeed, miR-1–expressing cells displayed impaired cell–cell attachment in 2D (Supplementary Fig. S2C) and 3D assays (Supplementary Fig. S2D). Moreover, miR-1 expression reduced infiltration in a 3D collagen matrix with cells displaying a cuboidal, noninvasive morphology (Fig. 3A with insets). Reduced migration was also confirmed by a wound-healing assay (Supplementary Fig. S2E). In contrast to the effects on migration, there was no effect of miR-1 on the cell cycle (with the exception of a small but nonsignificant increase in the apoptotic fraction in U87 cells (Supplementary Fig. S2F). Interestingly, glioblastoma multiforme cells cultured in stem-like conditions had significantly impaired neurosphere formation upon miR-1 expression, both in stably infected (Fig. 3B) and in transiently transfected cells (Supplementary Fig. S2G). Therefore, miR-1 expression reduced glioblastoma multiforme cell to cell and cell to matrix adhesion, leading to reduced neurosphere sizes and inhibited *in vitro* invasion.

The above results showed that miR-1 expression led to a variety of phenotypic changes. We thus hypothesized that miR-1 could be deregulating multiple signaling pathways linked to glioblastoma multiforme progression. We thus investigated the status of such oncogenic signaling in glioblastoma multiforme cells transfected with miR-1 and cultured either as monolayers or in "stem-like" neurosphere conditions. We observed reduced level of phospho-AKT (X12 only) but no changes in phospho-ERK levels (Fig. 3C). However phospho-JNK levels were consistently reduced, especially in stem-like conditions (where phospho-JNK levels were elevated). Stem-like culture conditions caused a significant increase in levels of the putative glioma stem cell marker CD133, as well as an increase in stem cell self-renewal factors BMI1 and SUZ12. Levels of the astrocyte lineage marker GFAP were significantly reduced under these neurosphere culture conditions. miR-1 transfection abrogated these effects of neurosphere culture and reduced levels of CD133, BMI1, and SUZ12 while increasing levels of differentiation marker GFAP (Fig. 3D). Interestingly, cells transferred from monolayer culture to stem-like conditions had significantly reduced endogenous expression of miR-1 (Supplementary Fig. S2H). Finally, we analyzed the effect of miR-1 expression on cellular receptors known to play a crucial role in glioblastoma multiforme cell biology. We observed elevated levels of the known miR-1 target MET (30, 31) under neurosphere conditions. As expected, pro-MET, MET, and phospho-MET levels were significantly reduced by miR-1 expression. Also, EGFR level was diminished in miR-1 expressing cells, whereas PDGFR level was increased in U87 and reduced in X12 cells, suggesting cell-type–specific effects (Fig. 3E). These results thus indicated that miR-1 inhibited multiple signaling pathways, associated with "stemness" of glioblastoma multiforme stem-like cells.

miR-1 expression blocks extracellular vesicle stimulation of glioblastoma multiforme invasion and growth

The findings showing reduced invasion and angiogenesis in miR-1–expressing cells suggested that it influences the tumor microenvironment. Thus, we hypothesized that miR-1 could be acting on intercellular communication via extracellular vesicles, which have been shown to be important mode of release biomolecules by glioblastoma multiforme cells (13). To investigate the role of paracrine communication via extracellular vesicles in neovascularization, we used a tube formation assay using recipient brain microvascular endothelial cells (32). These cells form tube-like structures in growth factor–supplemented medium (Fig. 4A, left). HBMVECs treated with glioblastoma multiforme neurosphere–derived extracellular vesicles (donor cells) formed significantly longer and more branched tube-like structures than controls. This effect was significantly reduced in the presence of extracellular vesicles collected from miR-1–expressing neurospheres compared with controls (Fig. 4A, right).

Next, we tested the effect of extracellular vesicles on migration of stem-like neurospheres. We found that the presence of extracellular vesicles (collected from donor neurospheres) strongly promoted recipient cell migration in spheroid assays (Fig. 4B). This effect was significantly diminished using extracellular vesicles collected from miR-1–expressing donor cells, both in terms of distance traveled by the cells and number of cells leaving the spheroid core (Fig. 4B, Supplementary Fig. S3A). We also found that extracellular vesicles derived from control neurosphere donor cells promoted neurosphere formation of recipient cells; whereas extracellular vesicles collected from miR-1–expressing donor cells had no significant effect (Fig. 4C). Expression of miR-1 in recipient cells also

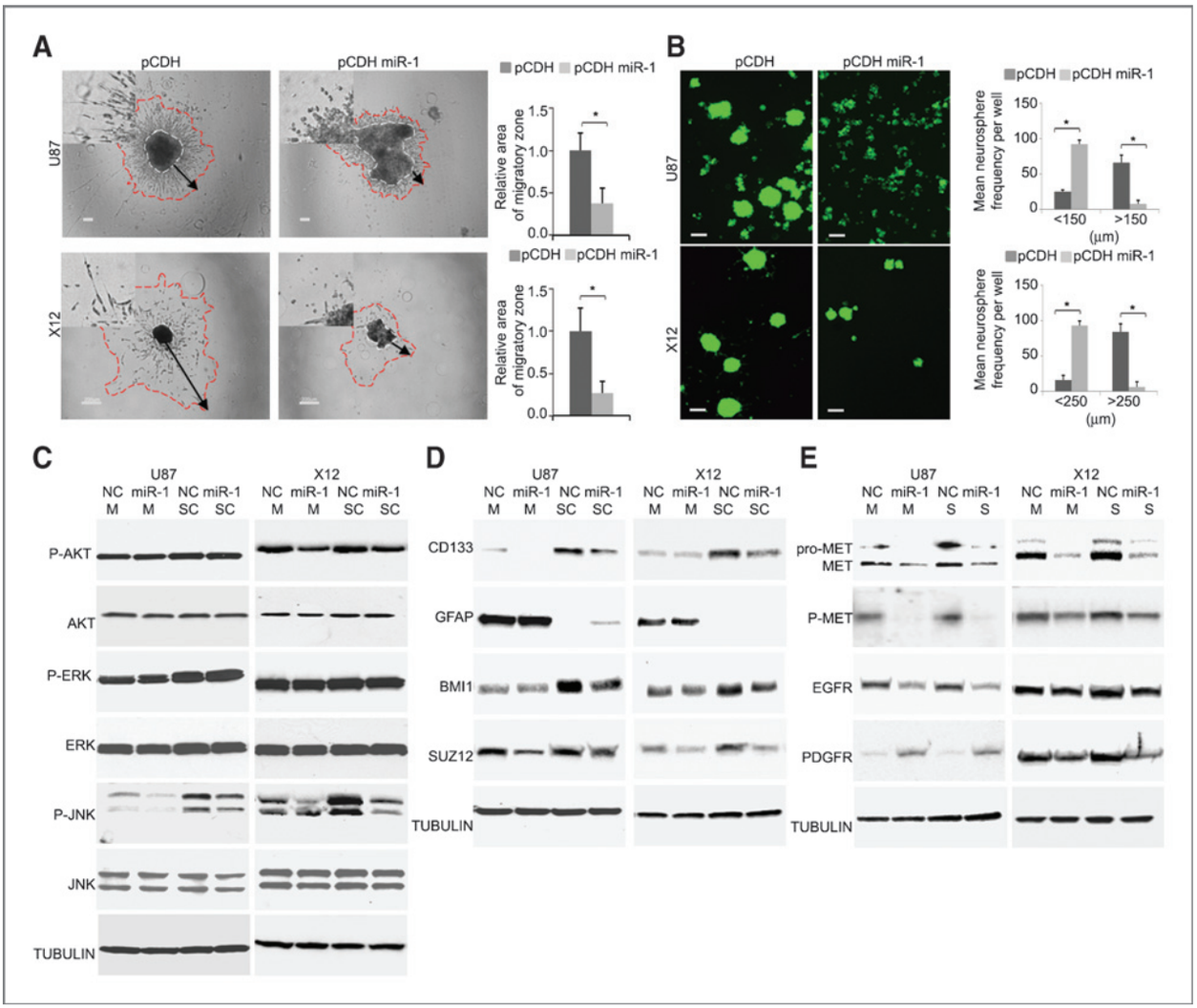

Figure 3. Overexpression of miR-1 in glioblastoma multiforme cells impairs cell–cell adhesion, spheroid migration, and neurosphere formation by affecting multiple effectors. A, migration of glioblastoma multiforme cells was measured by a spheroid dispersal assay. Representative images of spheroid migration of U87 (top) and X12 (bottom) glioblastoma multiforme cells transiently transfected with either negative control miR (NC) or miR-1. Scale bars, 100 μm (top) and 200 μm (bottom). The insets in all panels are magnified ×2.5. Migratory zones were quantified after indicated time, expressed as mean ± SD. *, $P < 0.05$. B, neurosphere formation capacity was determined by a self-renewal assay. Representative images of U87 and X12 cells stably expressing pCDH-GFP control vector (pCDH) or pCDH-GFP miR-1 vector (pCDH miR-1). Scale bars, 200 μm. Neurospheres were quantified after 72 hours, expressed as mean frequency of colony size by diameter divided into two classes ± SD. *, $P < 0.05$. C, cellular signaling was monitored by Western blot analysis of U87 and X12 cell lines cultured as monolayer (M) or stem cell-like neurospheres (SC). Cells were transiently transfected with either negative control miR (NC) or miR-1. Cell lysates were blotted with anti-phospho-specific antibodies and compared with total kinase antibodies. Tubulin was used as a loading control. D, stemness was monitored by Western blot analysis of U87 and X12 cell lines cultured as monolayer (M) or stem cell-like neurospheres (SC). Cells were transiently transfected with either negative control miR (NC) or miR-1. Cell lysates were blotted with indicated antibodies. Tubulin was used as a loading control. E, expression of cellular receptors was monitored by Western blot analysis of U87 and X12 cell lines cultured as monolayer (M) or stem cell-like neurospheres (SC). Cells were transiently transfected with either negative control miR (NC) or miR-1. Cell lysates were blotted with anti-phospho-specific antibodies and with total protein antibodies. Tubulin was used as a loading control.

prevented extracellular vesicle promotion of neurosphere formation (Supplementary Fig. S3B). Thus expression of miR-1 prevents extracellular vesicle stimulation of angiogenesis, invasion, and neurosphere formation in recipient cells.

As a control, we confirmed that miR-1 expression did not alter expression of the extracellular vesicle marker CD63 (Supplementary Fig. S3C). Interestingly, miR-1 expression did lead to a small but significant decrease in extracellular vesicle size (Supplementary Fig. S3D), but miR-1 expression did not alter the number of extracellular vesicles secreted by glioblastoma multiforme cells (Supplementary Fig. S3E). Additional characterization of extracellular vesicles released by glioblastoma multiforme stem-like cells showed that extracellular vesicle fractions lacked larger RNAs compared with total cellular RNA (Supplementary Fig. S3F) and that extracellular vesicles collected from miR-1–expressing cells showed

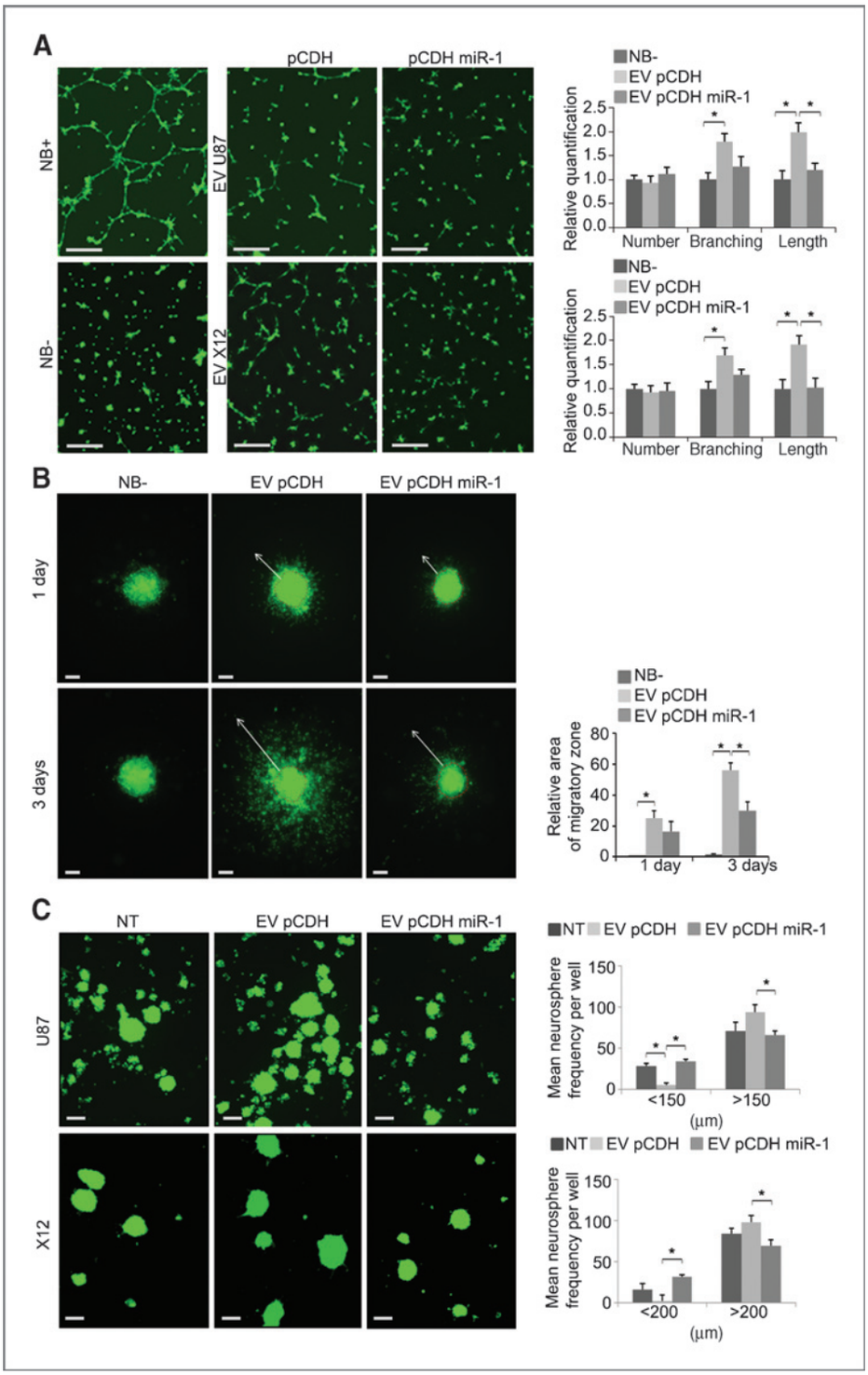

Figure 4. The extracellular vesicle–dependent phenotype is mitigated by miR-1. A, tube-like formation of HBMVECs in unsupplemented (NB−) and supplemented (NB+) neurobasal medium and upon the presence of extracellular vesicles in NB− medium was monitored by 3D Matrigel assay. Extracellular vesicles were collected from U87 (EV U87) and X12 (EV X12) cells stably infected with either pCDH-GFP control vector (pCDH) or pCDH-GFP miR-1–expressing vector (pCDH miR-1). Representative images are shown. Scale bars, 250 μm. Data, mean ± SD; *, $P < 0.05$. B, migration of glioblastoma multiforme stem-like neurospheres in NB− medium upon the presence of extracellular vesicles was measured by spheroid dispersal assay. Representative images of X12 spheroid migration after indicated time are shown. Extracellular vesicle were collected from X12 cells stably expressing pCDH-GFP control vector (EV pCDH) or pCDH-GFP miR-1 vector (EV pCDH miR-1). Scale bars, 100 μm. Migratory zones were quantified after indicated time, expressed as mean ± SD. *, $P < 0.05$. C, neurosphere formation capacity in the presence of extracellular vesicles was determined by self-renewal assay. Representative images of GFP-labeled U87 and X12 cells either nontreated (NT) or cultured in the presence of extracellular vesicles are shown. Extracellular vesicles were collected from corresponding cell lines stably expressing pCDH-GFP control vector (EV pCDH) or pCDH-GFP miR-1 vector (EV pCDH miR-1). Scale bars, 200 μm. Neurospheres were quantified after 72 hours, expressed as mean frequency of colony size by diameter divided into two classes ± SD. *, $P < 0.05$.

increased levels of RNAs smaller than 40 nt (Supplementary Fig. S3G). Therefore, we conclude that observed effects of extracellular vesicles derived from miR-1–expressing donor cells on recipient cells were more likely due to such extracellular vesicle cargo and not to a difference in extracellular vesicle quantity or release from donor cells.

miR-1 is transferred between glioblastoma multiforme cells by extracellular vesicle transport

We next asked whether miR-1 itself could be transferred by glioblastoma multiforme–derived extracellular vesicles. To visualize extracellular vesicle transfer, we created cell lines expressing RFP-CD63 and used them as donor cells.

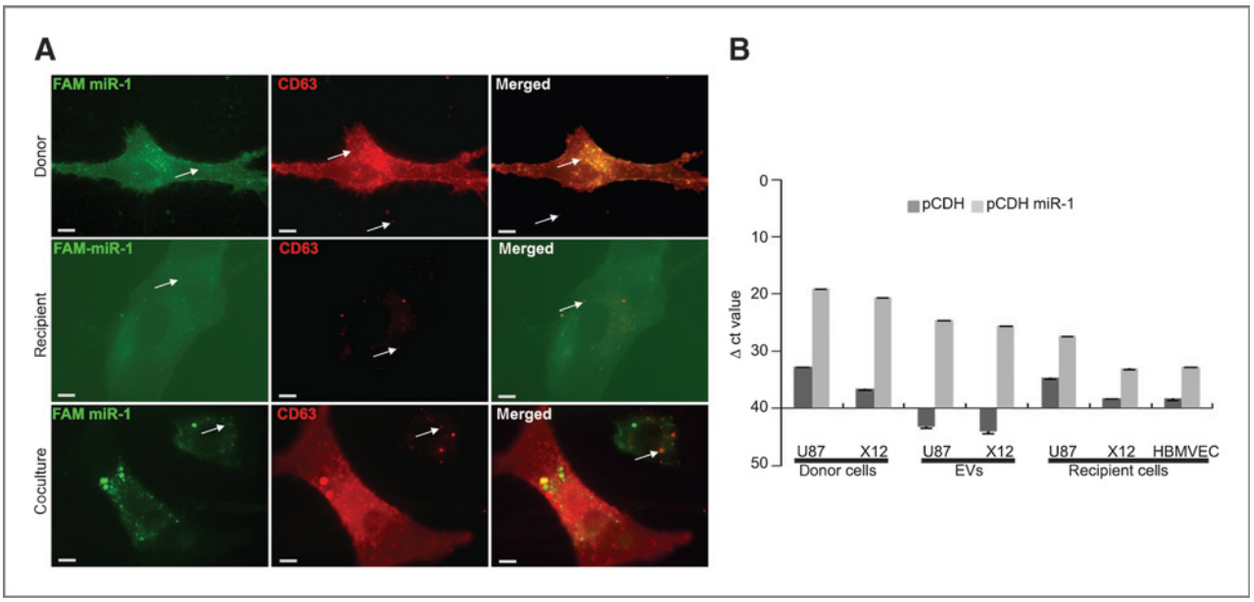

Figure 5. MiR-1 is transferred between glioblastoma multiforme cells by extracellular vesicle transport. A, uptake of glioblastoma multiforme–derived extracellular vesicles was monitored using co-labeled extracellular vesicles and miR. Donor U87 cells were stably infected with lentiviral particles of RFP-CD63 and transiently transfected with FAM labeled miR-1. Representative images show partial colocalization of miR-1 (green) and extracellular vesicles (red) in donor cells (top), in recipient U87 cells treated with extracellular vesicles from donor cells (middle), and in donor and recipient cells in coculture (bottom). Scale bars, 50 μm. Arrows indicate FAM signal alone (left), RFP signal alone (middle), and both signals colocalized (right). B, expression of miR-1 in donor cells, extracellular vesicles, and recipient cells was validated by qPCR. RNA was isolated from donor cells (U87, X12) stably infected with either pCDH-GFP control vector (pCDH) or pCDH-GFP miR-1 expressing vector (pCDH miR-1), extracellular vesicles collected from donor cells, and recipient U87, X12, and HBMVEC cells upon the treatment with extracellular vesicles. Data are shown as the mean raw ΔC_t value ± SD.

After treatment with extracellular vesicles derived from RFP-CD63–expressing cells, we detected RFP inside GFP-labeled recipient cells (Supplementary Fig. S4A). To visualize miR-1 transfer, we used U87 cells cotransfected with FAM-labeled miR-1 and RFP-labeled CD63 as extracellular vesicle donor cells. We observed that a substantial fraction of FAM-miR-1 co-localized with RFP-CD63 but also that a fraction of FAM-miR-1 remained in the donor cells cytoplasm (Fig. 5A, top). Extracellular vesicles released by FAM-miR-1/RFP-CD63–transfected cells were then added to recipient, nonfluorescent U87 cells. We observed partial colocalization of FAM-miR-1 with RFP-CD63 in the cytoplasm of recipient cells (Fig. 5A, middle; Supplementary Fig. S4B). A similar result was observed in coculture experiments (Fig. 5A, bottom), strongly suggesting that miR-1 can be transferred between cells through extracellular vesicles. To survey the transfer of miR-1 from donor to recipient cells, we conducted qPCR analysis on RNA extracted from donor cells (U87, X12), as well as their corresponding extracellular vesicles and recipient cells. We observed a significant increase of mature miR-1 levels in all tested samples (Fig. 5B), but the primary transcript was not altered in recipient cells (Supplementary Fig. S4C). This suggests that the observed increase of mature miR-1 levels in recipient cells is due to extracellular vesicle transfer not to increased endogenous miR-1 expression. These observations support the notion that the miR-1–dependent paracrine effect is at least partially mediated via extracellular vesicle transfer.

miR-1 overexpression affects the extracellular vesicle protein cargo by direct and indirect targeting

The extracellular vesicle–mediated phenotype observed in recipient cells suggested an active role of the extracellular vesicle molecular cargo. As miRs modulate the cellular proteome, we characterized the extracellular vesicle protein cargo in miR-1–expressing cells by global mass spectrometric analysis of extracellular vesicles. We identified 1,038 proteins, of which 462 were significantly downregulated and 11 upregulated in miR-1–expressing U87 cells compared with controls (Fig. 6A, Supplementary Table S1). "RNA binding" and "Vesicles" were among the most abundant functional annotations among these proteins and enzymes and transporters were among the most prominent types of proteins found in glioblastoma multiforme extracellular vesicles (Supplementary Fig. S5A and S5B). The most abundant networks identified were cancer-related and cell survival was among the most significant molecular process connected to proteins found in glioblastoma multiforme extracellular vesicles (Supplementary Table S2). Among identified proteins, 205 were putative targets of miR-1 and among these 84 were downregulated in extracellular vesicles collected from miR-1–expressing cells (Supplementary Fig. S5C and S5D). This was confirmed for three putative targets by Western blot analysis, which showed that ANXA2, FASN, and YWHAZ were significantly reduced in extracellular vesicles collected from miR-1–expressing cells (Fig. 6B). These results thus showed that miR-1 expression led to

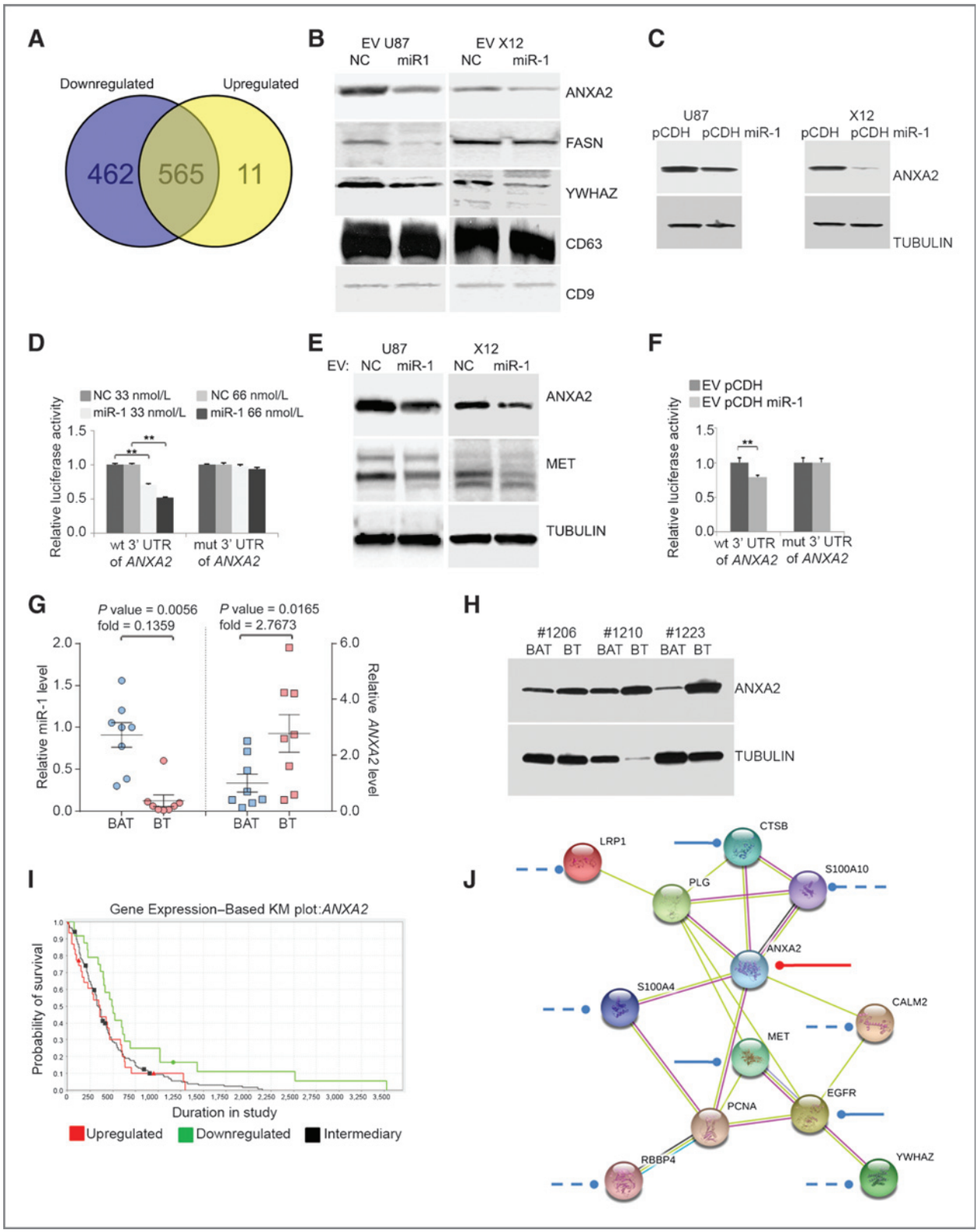

Figure 6. miR-1 directly targets EV ANXA2 overexpressed in human glioblastoma multiforme. A, Venn diagram depicting differential protein composition of extracellular vesicles derived from U87 cells stably infected with pCDH-GFP miR-1 expressing vector (downregulated, blue; upregulated, yellow) compared with EVs derived from U87 cells stably infected with pCDH-GFP control vector. (*Continued on the following page.*)

Table 1. Top deregulated molecules indentified in extracellular vesicles

Name	Hits NC/miR-1	Base2 log of ratio
ANXA2	1679/232	**2.9**
MYH9	709/107	**2.7**
FASN	99/1	**5.6**
UBA1	59/0	**5.9**
PRSS3	1/22	−3.5
IGHG4	0/11	−3.6
COL1A2	0/8	−3.2
LGALS7/LGALS7B	0/6	−2.8

NOTE: ANXA2 is the most abundant protein in glioblastoma multiforme–derived extracellular vesicles. List of top four (bold) deregulated extracellular vesicle proteins identified by mass spectrometry in extracellular vesicles derived from U87 cells transfected with either negative control (NC) or miR-1. The base 2 log of the ratio specifies the difference in number of peptide hits between the groups.

changes in the extracellular vesicle proteome, linked to cancer-related signaling networks.

Interestingly, *ANXA2* was identified as the most abundant extracellular vesicle protein (Table 1) and its mRNA 3′UTR contains a conserved miR-1 target site (Supplementary Fig. S5E). ANXA2 was previously implicated as an important pro-oncogenic factor in glioblastoma multiforme, promoting proliferation, invasion, and angiogenesis (20). The observed miR-1–dependent phenotype was thus consistent with ANXA2 downregulation, providing a biologic rationale for exploring a link between miR-1 and ANXA2. We thus proceed to verify the link between miR-1 and ANXA2. The level of ANXA2 in two cell lines stably expressing miR-1 was significantly reduced compared with that of controls (Fig. 6C). Similarly, downregulation of miR-1 was observed in a panel of five cell lines transfected with miR-1 (Supplementary Fig. S5F). Direct targeting of *ANXA2* by miR-1 was shown using a luciferase reporter assay with the 3′UTR of *ANXA2* and, in addition, mutagenesis of the predicted miR-1–binding site abolished the suppression of luciferase by miR-1 (Fig. 6D, Supplementary Fig. S5E). ANXA2 in conditioned medium was detected almost exclusively in the extracellular vesicle compartment (Supplementary Fig. S5G) and stem-like culture conditions caused a significant increase in ANXA2 levels, which was reflected in its extracellular vesicle content. This was strongly reduced by miR-1 expression (Supplementary Fig. S5H). These data thus confirmed that *ANXA2* was a direct mRNA target of miR-1 and that miR-1 expression resulted in decreased ANXA2 levels in extracellular vesicles.

To further show the functional consequences of extracellular vesicle-mediated miR-1 transfer, we analyzed its effect on ANXA2 in recipient cells. When purified extracellular vesicles collected from miR-1–expressing cells were added to recipient cells, there was a significant reduction of ANXA2 and MET proteins, when compared with treatment with control extracellular vesicles (Fig. 6E). As the endogenous level of mRNAs for these genes did not significantly change (data not shown), the observed downregulation was most likely due to expected microRNA-mediated effects during translation. The functionality of miR-1 in recipient cells was shown by a luciferase assay with the *ANXA2* 3′UTR reporter (Fig. 6F), showing a significant decrease in luciferase activity in cells treated with extracellular vesicles from miR-1–expressing cells. The effect was abolished by mutations in the miR-1 site of the *ANXA2* 3′UTR. These results strongly suggested that miR-1 delivered by extracellular vesicles is functional and can reduce ANXA2 levels in recipient cells by direct targeting of *ANXA2* 3′UTR.

To show the clinical relevance of miR-1/ANXA2 targeting in glioblastoma multiforme, we established that *ANXA2* mRNA

(*Continued*.) B, extracellular vesicle proteins were validated by Western blotting analysis. Extracellular vesicles were derived from U87 and X12 cells lines stably infected with either pCDH-GFP control vector (pCDH) or pCDH-GFP miR-1–expressing vector (pCDH miR-1). Extracellular vesicle lysates were blotted with specific antibodies against indicated proteins. CD9 and CD63 were used as a loading control. C, effects of miR-1 on the expression of ANXA2 were validated by Western blot analysis. U87 and X12 glioblastoma multiforme cell lines were stably expressing pCDH-GFP control vector (pCDH) or pCDH-GFP miR-1 expressing vector (pCDH miR-1). Cell lysates were blotted with antibodies against ANXA2. Tubulin was used as a loading control. D, direct targeting of *ANXA2* 3′UTR by miR-1 was validated using a luciferase/3′UTR reporter assay. COS7 cells were cotransfected with luciferase/*ANXA2* wild-type 3′UTR reporter vector (wt) and 33 or 66 nmol/L negative control miR (NC) or miR-1. A reporter vector with a mutated miR-1–binding site in the *ANXA2* 3′UTR (mut) was used as a control. Luciferase levels are expressed as mean relative to controls ± SD. **, $P < 0.01$. E, effects of extracellular vesicle–carried miR-1 on the expression of ANXA2 and MET were validated by Western blot analysis. U87 and X12 cells were exposed to the presence of extracellular vesicles derived from corresponding cells transiently transfected with either negative control miR (NC) or miR-1. Cell lysates were blotted with antibodies against ANXA2, MET, and tubulin was used as a loading control. F, direct targeting of *ANXA2* 3′UTR by EV-carried miR-1 was validated using luciferase/3′UTR reporter assay. U87 and X12 cells were exposed to the presence of extracellular vesicles derived from corresponding cells transiently transfected with either negative control miR (NC) or miR-1 and after 24 hours transfected with luciferase/*ANXA2* 3′UTR wild type (wt) and mutant (mut) reporter vector. Luciferase levels are expressed as mean relative to controls ± SD. **, $P < 0.01$. G, relative expression of miR-1 (left) and *ANXA2* mRNA (right) levels were validated by qPCR in glioblastoma multiforme brain tumor (BT) specimens versus matching brain adjacent to tumor (BAT; $n = 8$). Values, mean relative miR-1 expression level ± SD. H, ANXA2 protein level was validated in glioblastoma multiforme by Western blot analysis. Cell lysates from glioblastoma multiforme brain tumor (BT) specimens versus matching brain adjacent to tumor (BAT; $n = 3$) were blotted with antibodies against ANXA2. Tubulin was used as a loading control. I, association of *ANXA2* expression with patient survival [Kaplan–Meier (KM) plot] in glioblastoma multiforme. Data were obtained from The Cancer Genome Atlas. Upregulated ($n = 31$), downregulated ($n = 24$), and intermediary samples ($n = 156$) were analyzed. Up- versus downregulated, $P = 0.05$; upregulated versus intermediary, $P = 0.7134$; downregulated versus intermediary, $P = 0.0147$. J, miR-1–dependent targeting of EV ANXA2 network. ANXA2 partners were selected from extracellular vesicle proteins carried differentially in miR-1–dependent manner. Experimentally validated miR-1 targeting of ANXA2 is shown as a red line; targeting based on published data is shown as solid blue lines, and putative targeting based on target prediction software only is shown as a dashed lines. Networking was analyzed with STRING software.

levels were elevated in patient glioblastoma multiforme samples and were also significantly inversely correlated with miR-1 (Fig. 6G). Moreover, Western blot analysis showed a significant upregulation of ANXA2 protein in brain tumor samples (Fig. 6H). Also, according to Oncomine and TCGA databases, glioblastoma multiforme is characterized by high expression of *ANXA2* mRNA (Supplementary Fig. S5I), and its low expression is significantly associated with better outcome (Fig. 6I). Thus, these data strongly implicate ANXA2 as a significant player in glioblastoma multiforme biology and identify miR-1 as an important direct regulator of ANXA2, both in tumor cells and in the tumor microenvironment.

Discussion

Despite considerable progress in recent years, the regulation of signaling in the glioblastoma multiforme microenvironment is not well understood (7). Extracellular vesicle signaling via intercellular transport of proteins and RNAs, including miRs, is a recently discovered mechanism by which tumor cells, including glioblastoma multiforme, interact with their surroundings (12, 33). MiRs have been implicated in glioblastoma multiforme pathophysiology and therapy (34–36), but there are a limited number of studies showing the functional consequences of microRNA reintroduction to targeted cells in the context of the tumor microenvironment (37). As extracellular vesicles are capable of transporting nucleic acids (13, 38) and proteins as a part of physiologic intercellular communication, the approach of microRNA overexpression in donor cell may be used for their delivery. Here, we provide novel evidence that reintroduction of miR-1, important in antiproliferative, antiangiogenic, and anti-invasive action for glioblastoma multiforme, also contributes to microenvironmental remodeling by direct targeting of the glioblastoma multiforme cells' extracellular vesicle cargo. We also show for the first time that this remodeling is likely mediated by miR-1 targeting of ANXA2. These studies thus characterize glioblastoma multiforme's extracellular vesicle–mediated paracrine signaling network and identify some of the factors, such as miR1/ANXA2 that are relevant for known observed glioblastoma multiforme phenotypes.

Tumor-suppressive functions of miR-1 have been shown in numerous human malignancies (17, 39–41). Its action was associated with direct targeting of several oncogenes, including MET (30)—one of the crucial oncogenic drivers in glioblastoma multiforme. However, the role of miR-1 in glioblastoma multiforme has never been explored. Here we cross-referenced the results of 2 microRNA microarray analyses and found that the expression of miR-1 is significantly decreased in human glioblastoma multiforme patient samples compared with normal brain and is also downregulated in migrating cells, suggesting a role in glioblastoma multiforme growth and invasiveness. Upregulation of miR-1 expression in glioblastoma multiforme has far-reaching consequences for tumor phenotype, including diminished neurosphere formation capacity, *in vitro* tumor growth, angiogenesis, and invasiveness *in vivo*. Unexpectedly, we observed significantly reduced endothelial cell recruitment and neovascularization *in vivo*, suggesting microenvironmental alterations. Such a complex phenotype is likely to be mediated by multiple effectors. Restoration of miR-1 expression in glioblastoma multiforme cells is biologically consistent with our understanding of cancer as a disease of multiple aberrant signaling pathways that would thus require intervention at multiple levels (42). The fact that a single miR simultaneously downregulates a broad set of mRNA targets with potential pro-oncogenic properties provides a broad modulatory mechanism that may operate in other cancers as well as glioblastoma multiforme. Among a panel of oncogenic signaling kinases, the reduction of JNK activity, shown to play a crucial role in maintenance of self-renewal and tumorigenicity of glioblastoma multiforme stem cells (43, 44), was apparent. Also, stem cell factors known to play a vital role in glioblastoma multiforme stem cell maintenance such as CD133 or members of polycomb repressor complexes (36, 45) were significantly reduced upon miR-1 expression. Downregulation of MET and EGFR upon upregulation of miR-1 underlines its strong antitumorigenic effects. Here, for the first time, we describe targeting of MET by miR-1 in glioblastoma multiforme. *In silico* analysis suggested that the observed changes in the molecular milieu of miR-1–expressing glioblastoma multiforme cells are likely consequences of both direct and indirect effects.

The dramatic effect of miR-1 expression on blood vessel formation *in vivo* suggested complex tumor microenvironment rearrangements. This most likely was due to the altered secretion of pro-angiogenic factors and/or by the active release of overexpressed miR-1 into the microenvironment. Intercellular communication by extracellular vesicles was recently shown to contribute to horizontal cellular transformation, phenotypic reprogramming, and functional re-education of recipient cells via both local and systemic modification of microenvironment and direct transferring of biomolecules, including miRs (46). We characterized extracellular vesicles released by glioblastoma multiforme cells and found that miR-1 overexpressed in donor cells was in fact loaded into extracellular vesicles and transferred to recipient cells to functionally target its effectors there. Moreover, we showed that miR-1 is capable of microenvironmental modifications by affecting the molecular cargo of extracellular vesicles. Our results underline the functional role of glioblastoma multiforme–derived extracellular vesicles in tumorigenicity. The global proteomic analysis of extracellular vesicle content revealed the presence of more than a thousand proteins, among which ANXA2 was the most abundant. ANXA2 is an important oncogene in numerous cancers (47, 48), including glioblastoma multiforme where it high expression promoted growth, angiogenesis, and invasiveness, and correlated with poorer patient outcomes (20, 49). Interestingly, ANXA2 was among the most downregulated proteins in extracellular vesicles collected from miR-1 overexpressing cells. On the basis of the fact that the phenotype observed upon miR-1 expression is consistent with reduced levels of ANXA2, we hypothesized that this protein is not only the direct target of miR-1 but also its major effector in glioblastoma multiforme cells. Expression of miR-1 and *ANXA2* were inversely correlated in human glioblastoma multiforme samples, and miR-1 directly binds to site on the *ANXA2* 3′UTR,

leading to repression of ANXA2 protein levels. Furthermore, bioinformatic analysis revealed that miR-1 putatively targets several proteins functionally related to ANXA2 (Fig. 6J) in addition to previously published targeting of *MET* mRNA. miR-1 deregulated the protein cargo of glioblastoma multiforme–derived extracellular vesicles without significant differences in extracellular vesicle secretion or uptake, suggesting that observed phenotype is in fact mediated by differences in the content of extracellular vesicle molecular cargo, including ANXA2. These data strongly suggest a mechanistic link between miR-1 and ANXA2 suppression on glioblastoma multiforme cells and their microenvironment.

It has been postulated that miR replacement approaches have strong therapeutic potential because of the fact that single miRs can regulate multiple oncogenic pathways that are commonly deregulated in cancer (42). Our report provides novel evidence that miR-1 is inactivated in glioblastoma multiforme. Because miR-1 simultaneously targets major components of oncogenic signaling networks (JNK, PRCs, MET, EGFR, ANXA2), miR-1 loss may represent an important step in glioblastoma multiforme genesis and/or progression. Moreover, we showed that the pro-oncogenic impact that glioblastoma multiforme cells exert on their microenvironment by releasing extracellular vesicles is alleviated by miR-1. Thus the depletion of cellular and extracellular vesicle ANXA2 points toward miR-1 replacement as an attractive candidate for this therapeutic modality. These findings shed new light on the intricate communication networks in the glioblastoma multiforme microenvironment and open new possibilities for therapeutic intervention.

Disclosure of Potential Conflicts of Interest

No potential conflicts of interest were disclosed.

Authors' Contributions

Conception and design: A. Bronisz, F. Hochberg, S.E. Lawler, E.A. Chiocca, J. Godlewski

Development of methodology: A. Bronisz, Y. Wang, K.I. Ansari, G. De Rienzo, M. Mineo, J. Godlewski

Acquisition of data (provided animals, acquired and managed patients, provided facilities, etc.): Y. Wang, M.O. Nowicki, P. Peruzzi, K.I. Ansari, D. Ogawa, I. Nakano, J. Godlewski

Analysis and interpretation of data (e.g., statistical analysis, biostatistics, computational analysis): A. Bronisz, Y. Wang, L. Balaj, M. Mineo, S.E. Lawler, E.A. Chiocca, J. Godlewski

Writing, review, and/or revision of the manuscript: A. Bronisz, Y. Wang, P. Peruzzi, L. Balaj, M.C. Ostrowski, F. Hochberg, R. Weissleder, S.E. Lawler, E.A. Chiocca, J. Godlewski

Administrative, technical, or material support (i.e., reporting or organizing data, constructing databases): Y. Wang, E.A. Chiocca, J. Godlewski

Study supervision: E.A. Chiocca, J. Godlewski

Grant Support

This work was supported by NCI P01 (#108778; E.A. Chiocca, F. Hochberg, R. Weissleder) and an institutional sundry fund (E.A. Chiocca).

The costs of publication of this article were defrayed in part by the payment of page charges. This article must therefore be hereby marked *advertisement* in accordance with 18 U.S.C. Section 1734 solely to indicate this fact.

Received September 13, 2013; revised October 28, 2013; accepted November 17, 2013; published OnlineFirst December 5, 2013.

References

1. Hess KR, Broglio KR, Bondy ML. Adult glioma incidence trends in United States, 1977–2000. Cancer 2004;101:2293–9.
2. Stupp R, Mason WP, van den Bent MJ, Weller M, Fisher B, Taphoorn MJ, et al. Radiotherapy plus concomitant and adjuvant temozolomide for glioblastoma. N Engl J Med 2005;352:987–96.
3. Furnari FB, Fenton T, Bachoo RM, Mukasa A, Stommel JM, Stegh A, et al. Malignant astrocytic glioma: genetics, biology, and paths to treatment. Genes Dev 2007;21:2683–710.
4. Lefranc F, Brotchi J, Kiss R. Possible future issues in the treatment of glioblastomas: special emphasis on cell migration and the resistance of migrating glioblastoma cells to apoptosis. J Clin Oncol 2005; 23:2411–22.
5. Lathia JD, Heddleston JM, Venere M, Rich JN. Deadly teamwork: neural cancer stem cells and the tumor microenvironment. Cell Stem Cell 2011;8:482–5.
6. Calabrese C, Poppleton H, Kocak M, Hogg TL, Fuller C, Hamner B, et al. A perivascular niche for brain tumor stem cells. Cancer Cell 2007; 11:69–82.
7. Charles NA, Holland EC, Gilbertson R, Glass R, Kettenmann H. The brain tumor microenvironment. Glia 2011;59:1169–80.
8. Bonavia R, Inda MM, Cavenee WK, Furnari FB. Heterogeneity maintenance in glioblastoma: a social network. Cancer Res 2011;71: 4055–60.
9. van der Vos KE, Balaj L, Skog J, Breakefield XO. Brain tumor microvesicles: insights into intercellular communication in the nervous system. Cell Mol Neurobiol 2011;31:949–59.
10. Peinado H, Aleckovic M, Lavotshkin S, Matei I, Costa-Silva B, Moreno-Bueno G, et al. Melanoma exosomes educate bone marrow progenitor cells toward a pro-metastatic phenotype through MET. Nat Med 2012; 18:883–91.
11. Mittelbrunn M, Gutierrez-Vazquez C, Villarroya-Beltri C, Gonzalez S, Sanchez-Cabo F, Gonzalez MA, et al. Unidirectional transfer of microRNA-loaded exosomes from T cells to antigen-presenting cells. Nat Commun 2011;2:282.
12. Kucharzewska P, Christianson HC, Welch JE, Svensson KJ, Fredlund E, Ringner M, et al. Exosomes reflect the hypoxic status of glioma cells and mediate hypoxia-dependent activation of vascular cells during tumor development. Proc Natl Acad Sci U S A 2013; 110:7312–7.
13. Skog J, Wurdinger T, van Rijn S, Meijer DH, Gainche L, Sena-Esteves M, et al. Glioblastoma microvesicles transport RNA and proteins that promote tumour growth and provide diagnostic biomarkers. Nat Cell Biol 2008;10:1470–6.
14. Janga SC, Vallabhaneni S. MicroRNAs as post-transcriptional machines and their interplay with cellular networks. Adv Exp Med Biol 2011;722:59–74.
15. Ferdin J, Kunej T, Calin GA. Non-coding RNAs: identification of cancer-associated microRNAs by gene profiling. Technol Cancer Res Treat 2010;9:123–38.
16. Godlewski J, Newton HB, Chiocca EA, Lawler SE. MicroRNAs and glioblastoma; the stem cell connection. Cell Death Differ 2010;17: 221–8.
17. Nohata N, Hanazawa T, Enokida H, Seki N. microRNA-1/133a and microRNA-206/133b clusters: dysregulation and functional roles in human cancers. Oncotarget 2012;3:9–21.
18. Lokman NA, Ween MP, Oehler MK, Ricciardelli C. The role of annexin A2 in tumorigenesis and cancer progression. Cancer Microenviron 2011;4:199–208.
19. An JH, Lee SY, Jeon JY, Cho KG, Kim SU, Lee MA. Identification of gliotropic factors that induce human stem cell migration to malignant tumor. J Proteome Res 2009;8:2873–81.
20. Zhai H, Acharya S, Gravanis I, Mehmood S, Seidman RJ, Shroyer KR, et al. Annexin A2 promotes glioma cell invasion and tumor progression. J Neurosci 2011;31:14346–60.

21. Singh SK, Clarke ID, Terasaki M, Bonn VE, Hawkins C, Squire J, et al. Identification of a cancer stem cell in human brain tumors. Cancer Res 2003;63:5821–8.
22. Giannini C, Sarkaria JN, Saito A, Uhm JH, Galanis E, Carlson BL, et al. Patient tumor EGFR and PDGFRA gene amplifications retained in an invasive intracranial xenograft model of glioblastoma multiforme. Neuro-oncology 2005;7:164–76.
23. Godlewski J, Nowicki MO, Bronisz A, Nuovo G, Palatini J, De Lay M, et al. MicroRNA-451 regulates LKB1/AMPK signaling and allows adaptation to metabolic stress in glioma cells. Mol Cell 2010;37:620–32.
24. Williams SP, Nowicki MO, Liu F, Press R, Godlewski J, Abdel-Rasoul M, et al. Indirubins decrease glioma invasion by blocking migratory phenotypes in both the tumor and stromal endothelial cell compartments. Cancer Res 2011;71:5374–80.
25. Rothhammer T, Bataille F, Spruss T, Eissner G, Bosserhoff AK. Functional implication of BMP4 expression on angiogenesis in malignant melanoma. Oncogene 2007;26:4158–70.
26. Raposo G, Nijman HW, Stoorvogel W, Liejendekker R, Harding CV, Melief CJ, et al. B lymphocytes secrete antigen-presenting vesicles. J Exp Med 1996;183:1161–72.
27. Wisniewski JR, Zougman A, Nagaraj N, Mann M. Universal sample preparation method for proteome analysis. Nat Methods 2009;6:359–62.
28. Bronisz A, Sharma SM, Hu R, Godlewski J, Tzivion G, Mansky KC, et al. Microphthalmia-associated transcription factor interactions with 14-3-3 modulate differentiation of committed myeloid precursors. Mol Biol Cell 2006;17:3897–906.
29. Godlewski J, Nowicki MO, Bronisz A, Williams S, Otsuki A, Nuovo G, et al. Targeting of the Bmi-1 oncogene/stem cell renewal factor by microRNA-128 inhibits glioma proliferation and self-renewal. Cancer Res 2008;68:9125–30.
30. Datta J, Kutay H, Nasser MW, Nuovo GJ, Wang B, Majumder S, et al. Methylation mediated silencing of MicroRNA-1 gene and its role in hepatocellular carcinogenesis. Cancer Res 2008;68:5049–58.
31. Reid JF, Sokolova V, Zoni E, Lampis A, Pizzamiglio S, Bertan C, et al. miRNA profiling in colorectal cancer highlights miR-1 involvement in MET-dependent proliferation. Mol Cancer Res 2012;10:504–15.
32. Shao H, Chung J, Balaj L, Charest A, Bigner DD, Carter BS, et al. Protein typing of circulating microvesicles allows real-time monitoring of glioblastoma therapy. Nat Med 2012;18:1835–40.
33. Liu ZM, Wang YB, Yuan XH. Exosomes from murine-derived GL26 cells promote glioblastoma tumor growth by reducing number and function of CD8+T cells. Asian Pac J Cancer Prev 2013;14:309–14.
34. Ferretti E, De Smaele E, Miele E, Laneve P, Po A, Pelloni M, et al. Concerted microRNA control of Hedgehog signalling in cerebellar neuronal progenitor and tumour cells. EMBO J 2008;27:2616–27.
35. Kefas B, Godlewski J, Comeau L, Li Y, Abounader R, Hawkinson M, et al. microRNA-7 inhibits the epidermal growth factor receptor and the Akt pathway and is down-regulated in glioblastoma. Cancer Res 2008;68:3566–72.
36. Peruzzi P, Bronisz A, Nowicki MO, Wang Y, Ogawa D, Price R, et al. MicroRNA-128 coordinately targets Polycomb Repressor Complexes in glioma stem cells. Neuro-oncology 2013;15:1212–24.
37. Bronisz A, Godlewski J, Wallace JA, Merchant AS, Nowicki MO, Mathsyaraja H, et al. Reprogramming of the tumour microenvironment by stromal PTEN-regulated miR-320. Nat Cell Biol 2012;14:159–67.
38. Katakowski M, Buller B, Zheng X, Lu Y, Rogers T, Osobamiro O, et al. Exosomes from marrow stromal cells expressing miR-146b inhibit glioma growth. Cancer Lett 2013;335:201–4.
39. Fleming JL, Gable DL, Samadzadeh-Tarighat S, Cheng L, Yu L, Gillespie JL, et al. Differential expression of miR-1, a putative tumor suppressing microRNA, in cancer resistant and cancer susceptible mice. PeerJ 2013;1:e68.
40. Hudson RS, Yi M, Esposito D, Watkins SK, Hurwitz AA, Yfantis HG, et al. MicroRNA-1 is a candidate tumor suppressor and prognostic marker in human prostate cancer. Nucleic Acids Res 2012;40:3689–703.
41. Nasser MW, Datta J, Nuovo G, Kutay H, Motiwala T, Majumder S, et al. Down-regulation of micro-RNA-1 (miR-1) in lung cancer. Suppression of tumorigenic property of lung cancer cells and their sensitization to doxorubicin-induced apoptosis by miR-1. J Biol Chem 2008;283:33394–405.
42. Bader AG, Brown D, Winkler M. The promise of microRNA replacement therapy. Cancer Res 2010;70:7027–30.
43. Matsuda K, Sato A, Okada M, Shibuya K, Seino S, Suzuki K, et al. Targeting JNK for therapeutic depletion of stem-like glioblastoma cells. Sci Rep 2012;2:516.
44. Yoon CH, Kim MJ, Kim RK, Lim EJ, Choi KS, An S, et al. c-Jun N-terminal kinase has a pivotal role in the maintenance of self-renewal and tumorigenicity in glioma stem-like cells. Oncogene 2012;31:4655–66.
45. Abdouh M, Facchino S, Chatoo W, Balasingam V, Ferreira J, Bernier G. BMI1 sustains human glioblastoma multiforme stem cell renewal. J Neurosci 2009;29:8884–96.
46. Rak J. Extracellular vesicles - biomarkers and effectors of the cellular interactome in cancer. Front Pharmacol 2013;4:21.
47. Hedhli N, Falcone DJ, Huang B, Cesarman-Maus G, Kraemer R, Zhai H, et al. The annexin A2/S100A10 system in health and disease: emerging paradigms. J Biomed Biotechnol 2012;2012:406273.
48. Mussunoor S, Murray GI. The role of annexins in tumour development and progression. J Pathol 2008;216:131–40.
49. Gao H, Yu B, Yan Y, Shen J, Zhao S, Zhu J, et al. Correlation of expression levels of ANXA2, PGAM1, and CALR with glioma grade and prognosis. J Neurosurg 2013;118:846–53.